Published in final edited form as:
*Angew Chem Int Ed Engl*. 2010 April 6; 49(16): 2865–2868. doi:10.1002/anie.200905805.

# Plasmonic Modulation of the Upconversion Fluorescence in $NaYF_4$:Yb/Tm Hexaplate Nanocrystals using Gold Nanoparticles or Nanoshells**

**Hua Zhang**,
Department of Materials Science and Engineering, University of California, Los Angeles, CA 90095, U. S. A

**Yujing Li**,
Department of Materials Science and Engineering, University of California, Los Angeles, CA 90095, U. S. A

**Ivan A. Ivanov**,
Department of Chemistry and Biochemistry, University of California, Los Angeles, CA 90095, U. S. A

**Yongquan Qu**,
Department of Chemistry and Biochemistry, University of California, Los Angeles, CA 90095, U. S. A

**Yu Huang**, and
Department of Materials Science and Engineering, University of California, Los Angeles, CA 90095, U. S. A. California Nanosystems Institute, University of California, Los Angeles, CA 90095, U. S. A

**Xiangfeng Duan**
Department of Chemistry and Biochemistry, University of California, Los Angeles, CA 90095, U. S. A. California Nanosystems Institute, University of California, Los Angeles, CA 90095, U. S. A

Hua Zhang: yhuang@seas.ucla.edu; Yujing Li: yhuang@seas.ucla.edu; Ivan A. Ivanov: xduan@chem.ucla.edu; Yongquan Qu: xduan@chem.ucla.edu; Yu Huang: yhuang@seas.ucla.edu; Xiangfeng Duan: xduan@chem.ucla.edu

## Keywords

upconversion (UC); nanoparticles (NPs); metal-enhanced fluorescence (MEF); plasmonic resonance (PR); surface plasmon coupled emission (SPCE)

The ability to tune the spectral properties of rare-earth element doped upconversion nanocrystals (NCs), which can emit light at shorter wavelengths than the excitation source, are of considerable interest for biomedical imaging and therapeutics.[1–5] Nanoscale integration of multiple functional components can enable exciting new opportunities to precisely control and fine tune the electronic and optical properties of the resulting materials. Here we report a new approach to modulate upconversion emission through

**X.D. acknowledges partial support by the NIH Director's New Innovator Award Program, part of the NIH Roadmap for Medical Research, through grant number 1DP2OD004342-01. Confocal laser scanning microscopy was performed at the CNSI Advanced Light Microscopy/Spectroscopy Shared Resource Facility at UCLA, supported with funding from NIH-NCRR shared resources grant (CJX1-443835-WS-29646) and NSF Major Research Instrumentation grant (CHE-0722519).

Correspondence to: Yu Huang, yhuang@seas.ucla.edu; Xiangfeng Duan, xduan@chem.ucla.edu.

Supporting information for this article is available on the WWW under http://www.angewandte.org or from the author.

hetero-integration of the upconversion NCs with plasmonic gold nanostructures. Our studies show that gold nanoparticles (NPs) can be attached onto the upconversion NCs with variable density, which can then function as the nucleation seeds for the growth of continuous gold nanoshells. The attachment of gold NPs is found to greatly enhance the upconversion emission. Spectroscopic studies show that this enhancement has a strong spectral dependence with significantly larger enhancement factor near plasmon resonance frequency, suggesting that the surface plasmon coupled emission plays an important role in the enhancement of upconversion emission. On the contrary, gold nanoshells can greatly suppress the emission possibly due to the strong scattering of excitation irradiation. These findings open a new pathway to rationally modulate the upconversion emission, and can broadly impact areas such as biomedical imaging, sensing and therapeutics, as well as enable new opportunities for energy harvesting and conversion.

Surface plasmon resonance (SPR) is the collective electron cloud oscillation on a metal surface or NP caused by its interaction with incident light.[6,7] This leads to a number of interesting optical events such as the absorption and scattering of photons of certain wavelength and is responsible for the wide range of colors observed in metal nanoparticle colloids.[8,9] Additionally, the large local electrical fields generated by SPR in the vicinity of the NPs can significantly modify the spectroscopic properties of neighbouring fluorophores.[10–12] SPR is largely responsible for surface enhanced Raman spectroscopy (SERS) with an enhancement factor of up to $10^{14}$–$10^{15}$, allowing the technique to be sensitive enough for single molecule detection.[13–15] Recently, gold and silver NPs, or islands, have been explored to modulate fluorescent emission from various nanostructures such as semiconductor quantum dots or fluorescent molecules.[16–18]

Our $NaYF_4$:Yb/Tm NCs were synthesized by thermal decomposition of rare-earth/sodium trifluoroacetate precursors in oleic acid and octadecene.[19] The as-synthesized NCs are terminated with oleic acid ligands and are hydrophobic. The attachment of gold NPs and the growth of gold nanoshells are typically carried out in aqueous solution, requiring the dispersion of the NCs into water. To this end, two steps of surface modification have been performed for gold seed attachment and gold shell growth (Scheme 1; see also Supporting Information). First, a ligand exchange process was done by using poly(acrylic acid) (PAA) as a multidentate ligand which displaces the original hydrophobic ligands on the NC surface. The resulting PAA coated NCs are typically negatively charged. To facilitate the subsequent attachment of the negatively charged gold NPs, an additional layer of poly(allylamine hydrochloride) (PAH) is coated onto the NC surface to render them positively charged. To ensure that each surface modification process was successful, Fourier transform infrared (FTIR) spectra were taken to confirm the additional existence of the $-COOH$ or $-NH_2$ groups (Supporting Information). To attach the gold NPs onto the NC surface, negatively charged gold NPs were first prepared separately and then mixed with the upconversion NC aqueous solution in proper ratio and allowed to age for a controlled time. Gold shell growth was then carried out by introducing additional gold precursor and reductant into the upconversion NC solution.

The microstructures, morphologies and composition of the $NaYF_4$:Yb/Tm NCs were characterized by a transmission electron microscope (TEM). The as-prepared upconversion NCs typically have a hexagonal structure with uniform size around 180 nm (Fig. 1a). The relatively uniform contrast in TEM image suggests the NCs are single crystals, which can be confirmed by high resolution TEM images and electron diffraction patterns (Supporting Information). With the attachment of gold NPs, an increasing number of darker specks can be observed, in which each dark speck corresponds to a gold NP on the upconversion NC surface (Fig. 1b, c). During the Au shell growth stage, these Au NPs function as the seeds for the nucleation of gold on the upconversion NC surface. As the reaction proceeds, the size

of the gold NPs grows rather quickly and eventually merges together to form a continuous shell (Fig. 1d–f).

The upconversion emission spectra of the NCs were collected in aqueous solution (~1 wt %) under 980 nm diode laser excitation with a power density of ~ 50 mW/cm$^2$. The emission spectra of the upconversion NCs during the seeding stage show a significant increase in emission intensity with increasing number of attached Au NPs, and an enhancement factor of more than 2.5 was achieved (Fig. 2a). On the other hand, during the gold shell growth stage, the evolution of emission spectra show that the emission intensity decreases substantially as the shell forms (Fig. 2b). These studies clearly demonstrate that the attachment of gold NPs on the upconversion NC surface can enhance the upconversion emission, while the formation of the continuous gold shell can quench the emission. Additionally, it is interesting to note that the emission enhancement by Au NPs is highly wavelength dependent, with the enhancement factors in violet/blue region much larger than that in the red region (Fig. 2c). Specifically, more than 150% increase in emission intensity is observed at 452 nm and 476 nm, while only ~50% increase is seen at 647 nm. On the other hand, the quenching of the emission by the gold shell has much less dependence on the wavelength, with the quenching factors remaining roughly the same for all emission peaks (Fig. 2d).

To confirm this modulation in emission intensity is indeed originated from individual upconversion NCs rather than any other complex effect in solution, we used confocal microscopy to investigate the upconversion emission from individual NCs. To this end, the NCs were first spin-coated onto a glass slide, and then cured in gold seed solution for Au NP attachment, while the upconversion emission was monitored with increasing curing time. To ensure that we compared emission from the exact same location, we used lithography to create alignment markers on the glass slide. The reflection image of the NCs on the glass slide shows well separated NCs or NC clusters (Fig. 3a). The SEM image of a similar sample prepared on silicon wafer further shows the NCs are either single NCs or a few NC clusters (Fig. 3b). The confocal fluorescence image (Fig. 3c–e) of the same sample at the same area shown in Figure 3a clearly shows strong upconversion emission from the NCs when excited with a 980 nm laser, with each bright spot in the image corresponding to emission from one or a few NCs. Importantly, the confocal images clearly show that the upconversion emission from individual NCs can be significantly enhanced with increasing curing time in gold seed solution, demonstrating that the enhancement can be attributed to individual NCs upon the attachment of gold NPs. Quantitative analysis of the confocal images shows that an intensity enhancement factor of c.a. 2.6 can be achieved (Fig. 3f), consistent with the results in Figure 2a.

The observed enhancement in the upconversion emission is in stark contrast to the usual perception that the presence of metal in close proximity can lead to quenching of the fluorescence emission. We suggest the enhancement effect by the gold NPs may be attributed to at least two possible factors: (1) an increase of excitation rate by local field enhancement (LFE): an enhancement of effective excitation flux caused by local field enhancement associated with plasmonic resonance; (2) an increase of emission rate by surface plasmon coupled emission (SPCE): an enhancement of emission efficiency due to the coupling of the upconversion emission with the NP plasmonic resonance which will effectively increase both the non-radiative and radiative decay rate. SPCE can occur when the emission band of the fluorophore overlaps with the plasmon resonance frequency of the metal nanostructures.[16] Importantly, both of these factors have been used to account for the metal-enhanced fluorescence (MEF) in quantum dots or fluorescent molecules.[17,18]

To understand the interplay between the emission in upconversion NCs and plasmon resonance in Au NPs, we have characterized the plasmon resonance properties of NC-NP conjugates using UV-vis absorption spectra. Importantly, UV-Vis spectra of the gold NPs and NC-NP conjugates show a resonance peak around 510 nm (Fig. 4a), consistent with the plasmon resonance frequencies observed in similar gold NPs.[20,21] Slight red-shift is observed with increasing density of gold NPs on NC surface, which is also consistent with previous observations that the SPR peak would red shift with the aggregation of gold NPs.[22–24] This plasmonic resonance frequency of gold NPs overlaps well with the two major emission peaks in the upconversion NCs (452 nm and 478 nm). Therefore, the gold NP SPR can effectively couple with the upconversion emission and can thus increase the radiative decay rate, emission efficiency and intensity. With a better plasmonic coupling near the plasmon resonance frequency, the SPCE also explains well why a larger enhancement factor is observed in violet/blue emission than in red emission (Fig. 2a, c). These studies suggest that SPCE plays an important role in the spectral dependent enhancement of upconversion emission, although other effects such as LFE may also contribute. On the other hand, when a continuous gold shell is formed, the SPR peak is shifted to near-infrared region (Fig. 4b), which is highly dependent on the thickness and geometry of the gold shell.[25–27] This shift of SPR reduces the SPCE and also significantly increases the scattering of excitation light at 980 nm, and thus reduces the effective excitation flux, leading to a quench of the upconversion emission. Additionally, the complete surrounding gold shell can also block the emission transmittance from the upconversion NCs.

To further study the SPCE effect in our upconversion NC-NP conjugates, we used time-correlated single photon counting (TCSPC) technique to characterize the fluorescence lifetime (Fig. 5). The lifetime measurement clearly shows that the fluorescence decay of the upconversion NCs with gold NPs (average lifetime ~21 ns, Fig. 5b) is faster than that of the upconversion NCs only (average lifetime ~28 ns, Fig. 5a). Additionally, it is interesting to note that the distribution of the lifetime is narrower for NC-NP conjugates than NC only. However, the exact reason for this change needs further investigation in future studies. This study confirms that the fluorescence decay rates are enhanced by the presence of gold NPs, supporting the argument that SPCE can lead to a faster radiative decay rate and enhanced emission efficiency and intensity.

In summary, we have reported a new approach to modulate upconversion emission through plasmonic interaction between the upconversion NCs and gold nanostructures. The attachment of the gold NPs onto upconversion NCs can more than double the upconversion emission intensity. This enhancement can be at least partly attributed to SPCE which can increase the radiative decay rate and emission efficiency, although further study will be necessary to fully elucidate the exact underlying mechanism. The formation of a gold shell can significantly suppress the emission due to considerable scattering of excitation irradiation. These findings open a general pathway to rationally modulate the upconversion emission and can broadly impact areas including biomedical imaging, therapeutics and energy conversion.

## Supplementary Material

Refer to Web version on PubMed Central for supplementary material.

## References

1. Wang LY, Yan RX, Huo ZY, Wang L, Zeng JH, Bao J, Wang X, Peng Q, Li YD. Angew Chem Int Ed. 2006; 44:6054.
2. Rijke FVD, Zijlmans H, Li S, Vail T, Raap AK, Niedbala RS, Tanke HJ. Nat Biotech. 2001; 19:273.

3. Hampl J, Hall M, Mufti NA, Yao YM, MacQueen DB, Wright WH, Cooper DE. Anal Biochem. 2001; 288:176. [PubMed: 11152588]
4. Lim SF, Riehn R, Ryu WS, Austin N. Nano Lett. 2006; 6:169. [PubMed: 16464029]
5. Chatterjee D, Rufaihah AJ, Zhang Y. Biomat. 2008; 29:937.
6. Eustis S, El-Sayed MA. Chem Soc Rev. 2006; 35:209. [PubMed: 16505915]
7. Barnes WL, Dereux A, Ebbesen TW. Nature. 2003; 424:824. [PubMed: 12917696]
8. Tao A, Sinsermsuksakul P, Yang P. Nat Nanotechnol. 2007; 2:435. [PubMed: 18654329]
9. Daniel MC, Astruc D. Chem Rev. 2004; 104:293. [PubMed: 14719978]
10. Le F, Brandl DW, Urzhumov YA, Wang H, Kundu J, Halas NJ, Aizpurua J, Nordlander P. ACS Nano. 2008; 2:707. [PubMed: 19206602]
11. Thomas KG, Kamat PV. Acc Chem Res. 2003; 36:888. [PubMed: 14674780]
12. Zhang J, Fu Y, Chowdhury MH, Lakowicz JR. Nano Lett. 2007; 7:2101. [PubMed: 17580926]
13. Nie S, Emory SR. Science. 1997; 275:1102. [PubMed: 9027306]
14. Mahmoud MA, El-Sayed MA. Nano Lett. 2009; 9:3025. [PubMed: 19585987]
15. Campion A, Kambhampati P. Chem Soc Rev. 1998; 27:241.
16. Lakowicz JR. Plasmonics. 2006; 1:5. [PubMed: 19890454]
17. Gryczynski I, Malicka J, Shen YB, Gryczynski Z, Lakowicz JR. J Phys Chem B. 2002; 106:2191.
18. Lakowicz JR. Anal Biochem. 2001; 298:1. [PubMed: 11673890]
19. Boyer JC, Cuccia LA, Capobianco JA. Nano Lett. 2007; 7:847. [PubMed: 17302461]
20. Link S, El-Sayed MA. J Phys Chem B. 1999; 103:4212.
21. Messinger BJ, Ulrich von Raben K, Chang RK, Barber PW. Phys Rev B. 1981; 24:649.
22. Eah SK, Jaeger HM, Scherer NF, Lin XM, Wiederrecht GP. Chem Phys Lett. 2004; 386:390.
23. Feldstein MJ, Keating CD, Liau Y, Natan MJ, Scherer NF. J Am Chem Soc. 1997; 119:6638.
24. Bai JW, Huang SX, Wang LY, Chen Y, Huang Y. J Mater Chem. 2009; 19:921.
25. Oldenburg SJ, Averitt RD, Westcott SL, Halas NJ. Chem Phys Lett. 1998; 288:243.
26. Wang H, Goodrich GP, Tam F, Oubre C, Nordlander P, Halas NJ. J Phys Chem B. 2005; 109:11083. [PubMed: 16852350]
27. Wang LY, Bai JW, Li YJ, Huang Y. Angew Chem Int Ed. 2008; 47:2439.

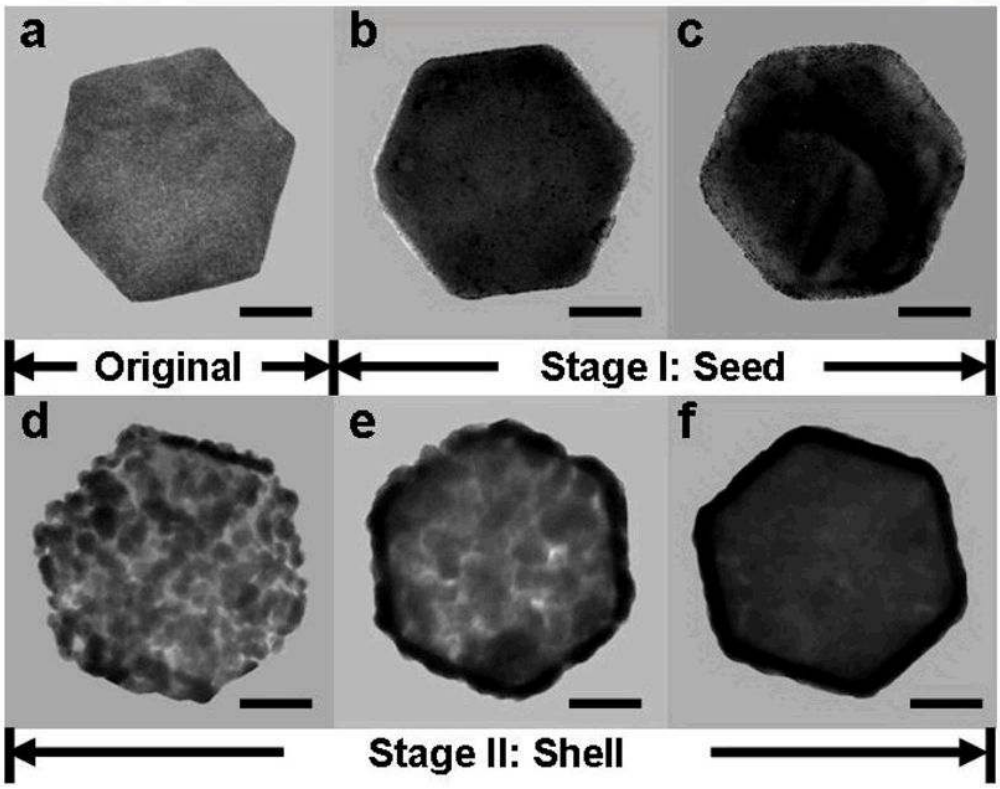


**Figure 1.**
Time lapse TEM images of the upconversion NCs during the process of gold seed attachment and shell growth, (a) original, (b–c) with increasing number of attached gold NPs and (d–f) with growing gold nanoshell (Scale Bar: 50 nm).

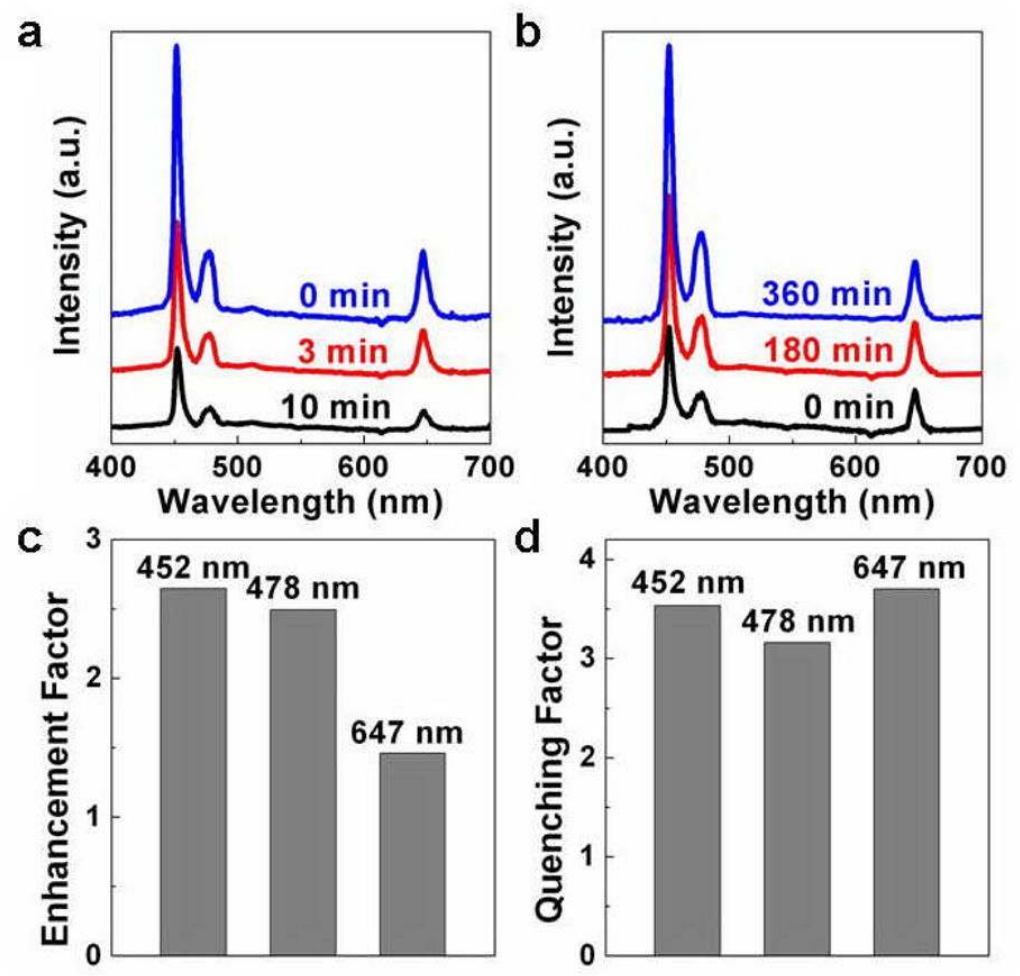


**Figure 2.**

Room temperature upconversion emission spectra of $NaYF_4$:Yb/Tm NCs during (a) gold seed attachment stage (0–360 min) and (b) gold shell growth stage (0–10 min). (c) Enhancement factors after gold NPs attachment and (d) quenching factors after gold shell growth at different emission wavelengths.

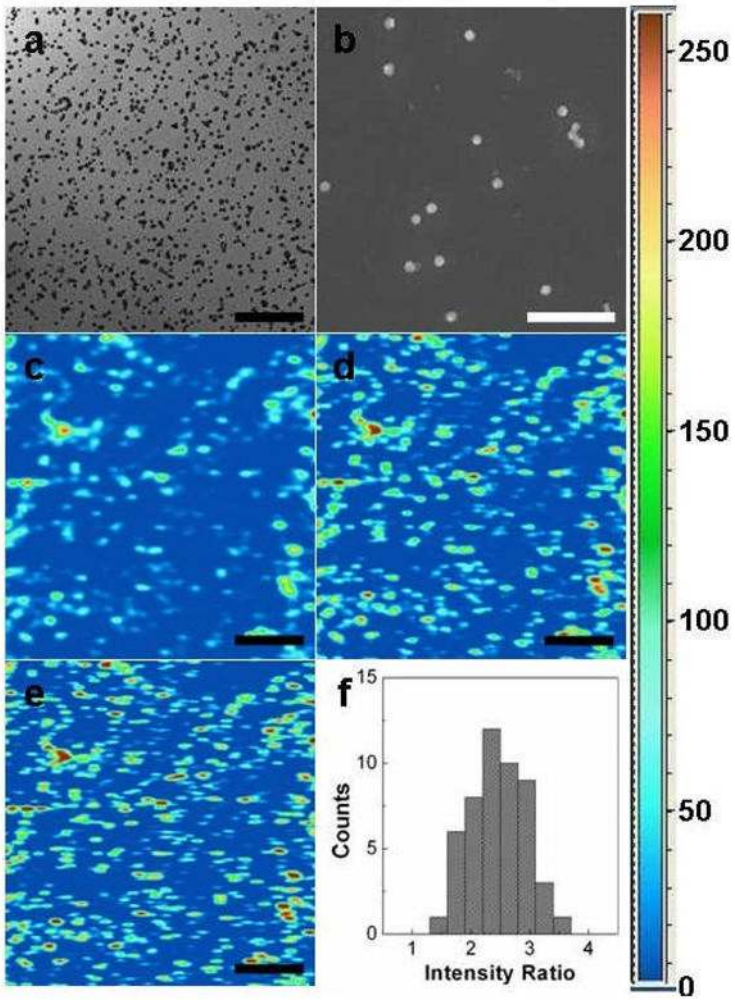


**Figure 3.**

(a) Reflection image of NCs on glass substrate. (b) SEM image of a similar sample prepared on silicon wafer. (c–e) Confocal upconversion fluorescence images of the upconversion NCs dipped into gold seed solution for (c) 0 min, (d) 180 min and (e) 360 min. (f) Histogram of the enhancement factors of 50 bright spots (intensity ratio between (e) and (c)). (Scale Bar: 3 μm for b and 20 μm for a, c, d and e)

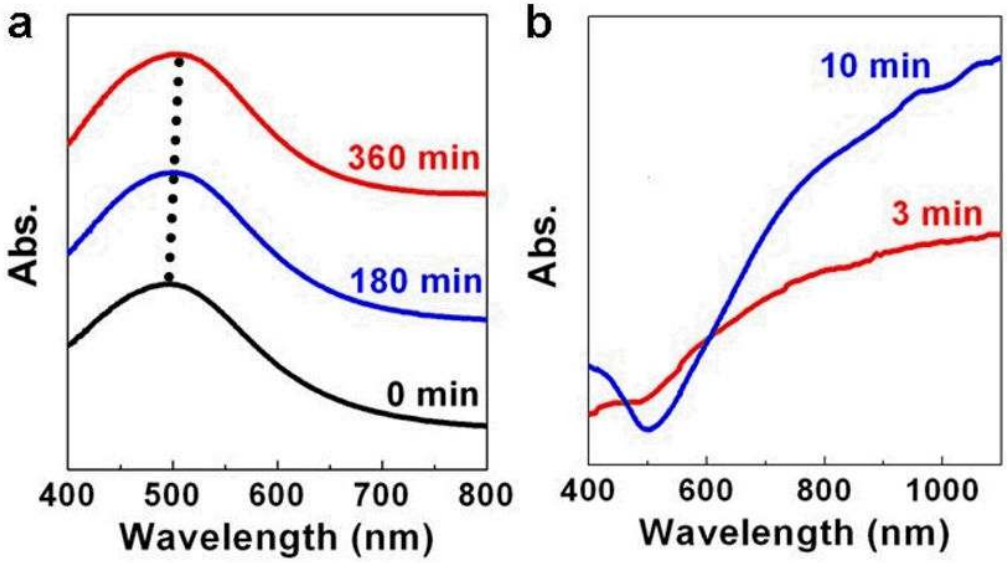


**Figure 4.**
UV-Vis spectra of upconversion NCs (a) with gold nanoseeds and (b) with gold shell at different times.

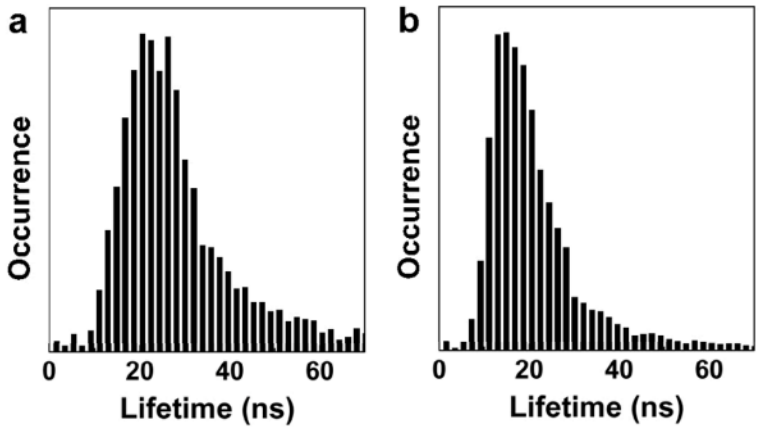


**Figure 5.**
Histograms of lifetimes of (a) upconversion NCs and (b) upconversion NCs with attached gold NPs.

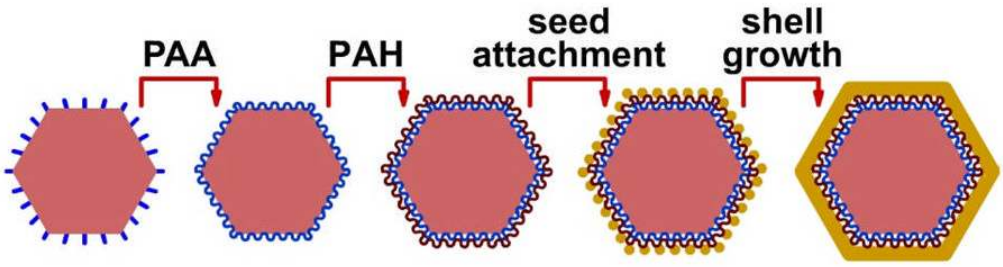


**Scheme 1.**
Schematic illustration of surface functionalization, gold NP attachment, and gold nanoshell growth on the upconversion NCs.